Trapping a Hydrazine Reduction Intermediate on the Nitrogenase Active Site†

Brett M. Barney,‡ Mikhail Laryukhin,§ Robert Y. Igarashi,‡ Hong-In Lee,§,|| Patricia C. Dos Santos,⊥ Tran-Chin Yang,§ Brian M. Hoffman,*,§ Dennis R. Dean,*,⊥ and Lance C. Seefeldt*,‡

Department of Chemistry and Biochemistry, Utah State University, Logan, Utah 84322, Department of Biochemistry, Virginia Tech, Blacksburg, Virginia 24061, Department of Chemistry, Northwestern University, Evanston, Illinois 60208, and Department of Chemistry Education, Kyungpook National University, Daegu 702-701, Korea

Received March 9, 2005; Revised Manuscript Received April 14, 2005

ABSTRACT: A major challenge in understanding the mechanism of nitrogenase, the enzyme responsible for the biological fixation of N_2 to two ammonias, is to trap a nitrogenous substrate at the enzyme active site in a state that is amenable to further characterization. In the present work, a strategy is described that results in the trapping of the substrate hydrazine (H_2N-NH_2) as an adduct bound to the active site metal cluster of nitrogenase, and this bound adduct is characterized by EPR and ENDOR spectroscopies. Earlier work has been interpreted to indicate that nitrogenous (e.g., N_2 and hydrazine) as well as alkyne (e.g., acetylene) substrates can bind at a common FeS face of the FeMo-cofactor composed of Fe atoms 2, 3, 6, and 7. Substitution of α-70^{Val} that resides over this FeS face by the smaller amino acid alanine was also previously shown to improve the affinity and reduction rate for hydrazine. We now show that when α-195^{His}, a putative proton donor near the active site, is substituted by glutamine in combination with substitution of α-70^{Val} by alanine, and the resulting doubly substituted MoFe protein (α-70^{Ala}/α-195^{Gln}) is turned over with hydrazine as substrate, the FeMo-cofactor can be freeze-trapped in a $S = {}^1/_2$ state in high yield (~70%). The presumed hydrazine−FeMo-cofactor adduct displays a rhombic EPR signal with $g = [2.09, 2.01, 1.93]$. The optimal pH for the population of this state was found to be 7.4. The EPR signal showed a Curie law temperature dependence similar to the resting state EPR signal. Mims pulsed ENDOR spectroscopy at 35 GHz using ^{15}N-labeled hydrazine reveals that the trapped intermediate incorporates a hydrazine-derived species bound to the FeMo-cofactor; in spectra taken at g_1 this species gives a single observed ^{15}N signal, $A(g_1) = 1.5$ MHz.

Nitrogenase is the enzyme responsible for the biological fixation (reduction) of dinitrogen, with the optimal reaction stoichiometry shown in the equation:

$$N_2 + 8e^- + 16MgATP + 8H^+ \rightarrow 2NH_3 + H_2 + 16MgADP + 16P_i \quad (1)$$

In the best studied form of nitrogenase, two component proteins work together to catalyze this reaction (*1*−*3*). The larger component, called the MoFe protein,[1] contains a 7Fe-9S-Mo-X-homocitrate cofactor (FeMo-cofactor) that provides the substrate-binding site (*4*, *5*), where the identity of X remains unknown but has been proposed to be N^{3-} (*6*−*9*). Progress toward understanding how substrates interact with the FeMo-cofactor has been made by freeze−quench experiments using alternative substrates or inhibitors under turnover conditions. These studies have included the trapping of turnover intermediates in which the FeMo-cofactor binds the inhibitor CO (*10*−*13*) or various alkynes (*14*−*16*) or CS_2 (*17*) as alternative substrates. It was recently shown that substitution of the MoFe protein amino acid α-70^{Val} by amino acids having either a smaller side chain (alanine) or larger side chain (isoleucine) increases or diminishes the size of substrates that can be accommodated at the active site for reduction (*18*, *19*). This was interpreted to indicate that the Fe 2, 3, 6, 7 face approached by the α-70^{Val} residue provides the substrate-binding site. The capacity to accommodate alkynes larger than C_2H_2 at the substrate-binding site made it possible to freeze−trap an intermediate in the reduction of the substituted alkyne, propargyl alcohol ($HC{\equiv}CCH_2OH$) (*14*, *15*, *18*, *20*). ENDOR characterization of this species showed it to be the reduction product, allyl alcohol ($H_2C{=}CHCH_2OH$), bound as a ferracycle (*14*) to a single Fe of that face, proposed to be Fe 6 (*20*, *21*). Analysis of the α-70^{Ile}-substituted MoFe protein, which is blocked for the reduction of all substrates tested except protons (*19*), has been interpreted to indicate that the above alkyne reduction

† This work was supported by grants from the National Institutes of Health (R01-GM59087 to L.C.S. and D.R.D.; HL13531 to B.M.H.) and the National Science Foundation (MCB-0316038 to B.M.H.) and by the National Research Initiative of the USDA Cooperative State Research, Education and Extension Service (2004-35318-14905 to B.M.B.).

* Address correspondence to these authors. L.C.S.: e-mail, seefeldt@cc.usu.edu; phone, 435-797-3964; fax, 435-797-3390. D.R.D.: e-mail, deandr@vt.edu; phone, 540-231-5895; fax, 540-231-7126. B.M.H.: e-mail, bmh@northwestern.edu; phone, 847-491-3104; fax, 847-491-7713.

‡ Utah State University.

§ Northwestern University.

|| Kyungpook National University.

⊥ Virginia Tech.

[1] Abbreviations: EPR, electron paramagnetic resonance; ENDOR, electron−nuclear double resonance; Fe protein, iron protein; MoFe protein, molybdenum−iron protein; FeMo-cofactor, iron−molybdenum cofactor.

10.1021/bi0504409 CCC: $30.25
Published on Web 05/11/2005

intermediate could be relevant to the mechanism of N_2 reduction.

To date, it has not been possible to trap an N_2 reduction intermediate in a concentration that is amenable to detailed quantitative spectroscopic analyses. As an alternative strategy, we here describe studies aimed at trapping a potential intermediate in the N_2 reduction pathway by using hydrazine (H_2N-NH_2) as a substrate. This approach was selected because the six electron/six proton reduction of N_2 to two ammonia has been proposed to proceed through metal-bound semireduced intermediate states electronically equivalent to diazene (HN═NH) and hydrazine (*22*−*26*). This proposal has received support from the detection of hydrazine following the acid quenching of nitrogenase during N_2 reduction (*23*) and the detection of trace amounts of hydrazine during the reduction of N_2 to ammonia by the vanadium-dependent nitrogenase (*27*, *28*). Nitrogenase reduces hydrazine by two electrons and two protons to yield two ammonia (*29*), but it is a relatively poor substrate. We recently reported that hydrazine is a much better substrate for nitrogenase (lowered K_m and increased V_{max}) when α-70^{Val} is substituted by alanine (*19*). In parallel studies to those in which we freeze-trapped a propargyl alcohol reduction intermediate (*14*, *15*, *19*, *20*), we now have used a combined biochemical−genetic strategy to trap a hydrazine-derived adduct bound to the FeMo-cofactor and describe the characterization of this species by EPR and ENDOR spectroscopies.

EXPERIMENTAL PROCEDURES

Materials and Protein Purification. All reagents were obtained from Sigma-Aldrich Chemicals (St. Louis, MO) and were used as provided unless otherwise specified. Hydrazine (^{14}N) was obtained as the dihydrate, while hydrazine (^{15}N-labeled) was obtained as the sulfate from Cambridge Isotopes (Andover, MA). *Azotobacter vinelandii* strains DJ995 (wild-type), DJ1310 (α-70^{Ala}), DJ997 (α-195^{Gln}), and DJ1316 (α-195^{Gln}/α-70^{Ala}) were prepared and grown, and nitrogenase proteins were expressed as described previously (*30*). The MoFe protein from each strain contained a seven-histidine tag on the α-subunit, allowing purification by a Zn affinity chromatography protocol (*30*). All proteins were obtained at greater than 95% purity as judged by SDS−PAGE analysis using Coomassie blue staining. Manipulation of proteins was done in septum-sealed serum vials under an argon atmosphere. All transfers of gases and liquids were done using gastight syringes.

Dinitrogen, Proton, and Hydrazine Reduction Assays. The rates for N_2 reduction were determined in 9 mL sealed vials with 1 mL liquid volume using established protocols for 10 min at 30 °C (*31*, *32*). The assay liquid contained a MgATP regeneration system (5 mM ATP, 6 mM $MgCl_2$, 30 mM phosphocreatine, and 0.2 mg/mL creatine phosphokinase) in a MOPS buffer (150 mM, pH 7.0) with 1.2 mg/mL BSA and 9 mM dithionite. Solutions were degassed with oxygen-free N_2, and the gas phase contained 1 atm of N_2. MoFe protein was added (100 μg) followed by Fe protein (500 μg) to initiate the reaction. The reaction was quenched by the addition of 300 μL of 400 mM EDTA. Ammonia was quantified by a liquid chromatographic−fluorescence method (*33*) with modifications (*19*). A 10 μL aliquot of postreaction solution containing NH_3 was added to 1 mL of a solution containing 20 mM phthalic dicarboxyaldehyde, 3.5 mM 2-mercaptoethanol, 5% (v/v) ethanol, and 200 mM potassium phosphate, pH 7.3, and allowed to react in the dark for 30 min. The mixture was injected and separated by HPLC on a C-18 guard column resolved isocratically with a 10 mM phosphate buffer at pH 7.3 containing 50% acetonitrile at a flow rate of 1.8 mL/min. Detection was by fluorescence ($\lambda_{excitation}/\lambda_{emission}$ of 410 nm/472 nm) with quantification by comparison to an NH_3 standard curve generated using NH_4Cl.

The rates for H^+ reduction were determined using the assay mixture described above, except that the gas phase consisted of argon. Dihydrogen in the headspace of quenched samples was determined by analysis with gas chromatography with a molecular sieve 5A column and a TCD detector. Hydrazine inhibition of proton reduction was determined in the buffer solution described above except that the pH was adjusted to 7.0 following the addition of hydrazine.

The rates of hydrazine reduction were determined from the ammonia formation using the fluorescent detection technique described above. The assay mixture was the same as described above except that 50 mM hydrazine was added and the final pH was adjusted to 7.7. The rates of MgATP hydrolysis were determined as previously described (*32*, *34*).

X-band EPR Sample Preparation and Analysis. Samples under turnover conditions were prepared in a reaction mixture containing a MgATP regeneration system (10 mM ATP, 15 mM $MgCl_2$, 20 mM phosphocreatine, and 0.2 mg/mL phosphocreatine kinase) in 200 mM MOPS buffer, pH 7.3, with 50 mM dithionite and 50 mM hydrazine. The MoFe protein concentration was ~75 μM in all samples. The reaction was initiated by the addition of 50 μM Fe protein. EPR samples under resting conditions were prepared as described above, except that Fe protein was not included. All X-band EPR samples were allowed to react at room temperature for approximately 30 s, followed by freezing in liquid nitrogen in 4 mm standardized quartz EPR tubes. For the pH profile, the same solution as described above was used, with the substitution of 50 mM MES, 50 mM TAPS, and 50 mM MOPS as buffer, and the pH was adjusted by the addition of HCl or NaOH. X-band EPR spectra were recorded using a Bruker ESP-300 E spectrometer with an ER 4116 dual-mode X-band cavity equipped with an Oxford Instruments ESR-900 helium flow cryostat. Spectra were obtained at a microwave frequency of 9.65 GHz. Precise values of the frequency were recorded for each spectrum to determine *g* alignment. Initial spectra were obtained at a power setting of 2.0 mW, with a modulation amplitude of 1.26 mT and a temperature of 8 K, and were the sum of five scans. Subsequent data manipulation was done using IGOR Pro (WaveMetrics, Lake Osewego, OR). The temperature dependence (4.8−15 K) of the EPR signal intensity was determined at 100 and 200 μW for the turnover and resting state signals, respectively, for the α-195^{Gln}/α-70^{Ala} MoFe protein. The microwave power dependence on EPR signal intensity was determined at 4.8 K with microwave powers from 10 μW to 2 mW.

35 GHz EPR/ENDOR Spectroscopy and Sample Preparation. Samples for 35 GHz EPR/ENDOR spectroscopy were prepared with [$^{14/15}N$]hydrazine as described above for the X-band EPR turnover samples, except that the concentrations of MoFe protein and Fe protein were tripled and the samples were frozen in Q-band EPR tubes. 35 GHz cw EPR spectra

Table 1: Specific Activities and Electron Fluxes for MoFe Proteins

	substrates[a]				
	proton[b]	N_2 (1 atm)[b]		hydrazine (50 mM)[c]	
	nmol of H_2 min^{-1} mg^{-1}	nmol of H_2 min^{-1} mg^{-1}	nmol of NH_3 min^{-1} mg^{-1}	nmol of H_2 min^{-1} mg^{-1}	nmol of NH_3 min^{-1} mg^{-1}
α-70^{Val}/α-195^{His}	2190 ± 90 (4380)	690 ± 60 (1380)	590 ± 15 (1770)	1480 ± 90 (2960)	320 ± 15 (320)
α-70^{Ala}/α-195^{His}	2040 ± 30 (4080)	1440 ± 40 (2880)	360 ± 20 (1080)	1170 ± 20 (2340)	1210 ± 10 (1210)
α-70^{Val}/α-195^{Gln}	1900 ± 30 (3800)	1060 ± 50 (2120)	5 ± 1 (15)	320 ± 10 (640)	30 ± 10 (30)
α-70^{Ala}/α-195^{Gln}	1330 ± 40 (2660)	1310 ± 40 (2620)	8 ± 3 (20)	200 ± 10 (400)	70 ± 20 (70)

[a] All assays were performed at 30 °C for 10 min at a MoFe protein to Fe protein ratio of 1:20 and are expressed per mg of MoFe protein. Electron flux going to the noted product is shown in parentheses as nmol of e^- min^{-1} mg^{-1}. [b] Proton and nitrogen reduction assays were performed at pH 7.0. [c] Hydrazine reduction assays were performed at pH 7.7.

(not shown) were recorded on a modified Varian E-110 spectrometer equipped with a helium immersion dewar at 2 K under "rapid passage" condition using 100 kHz field modulation (*35*). Q-band Mims three-pulse ENDOR spectra, pulse sequence $t_{mw}-\tau-t_{mw}-T(rf)-t_{mw}-\tau-$echo (*36*), were obtained at 2 K on a locally constructed spectrometer (*37*). To first order, the ENDOR spectrum of a ^{15}N coupled to an $S = {}^1/_2$ spin center (single orientation) is a doublet with frequencies given by $\nu_\pm = |\nu_N \pm A/2|$, where ν_N is the nuclear Larmor frequency and A is the orientation-dependent hyperfine coupling constant of the coupled nucleus.

RESULTS

Hydrazine as a Substrate and Inhibitor of Proton Reduction. During nitrogenase catalysis, total electron flux (electrons flowing through nitrogenase to all substrates) is relatively constant and independent of the substrate(s) present. Namely, available reducing equivalents are distributed between proton reduction and reduction of other substrates, depending upon the substrate being used. In the absence of any other substrate, all electron flux is directed toward proton reduction. Thus, the effectiveness for a particular substrate to interact with the active site can be evaluated by its capacity to inhibit proton reduction. Under the conditions used here, when hydrazine is used as substrate under saturating conditions for the wild-type MoFe protein, only ~10% of electron flux is diverted to hydrazine reduction with the balance going to proton reduction (Table 1) and with retention of maximal electron flux through nitrogenase (Table 2). Thus, hydrazine is a relatively poor substrate for the normal wild-type nitrogenase. It has previously been shown that the capacity for hydrazine to access the active site can be improved by substitution of the α-70^{Val} residue by α-70^{Ala} with a consequent 8-fold decrease in K_m and a doubling in V_{max}. This feature is also confirmed in Table 1 where it is shown that a higher percentage of electron flux is diverted to hydrazine reduction (34%) for the α-70^{Ala}-substituted MoFe protein when compared to the wild-type MoFe protein (~10%). Maximal electron flux through nitrogenase is not altered when hydrazine is presented to the α-70^{Ala} MoFe protein (Table 2). On the basis of these and related experiments involving the effect of substitution by either alanine or isoleucine at the α-70^{Val} position on the reduction of N_2, acetylene, or hydrazine, it was proposed that all of these substrates bind and are reduced at the Fe-S face within the FeMo-cofactor that is approached by the α-70^{Val} side chain (*19*).

Previous work has shown that substitution by glutamine of the α-195^{His} residue, located near the proposed substrate-binding face of the FeMo-cofactor (Figure 1), decreases the capacity for N_2 reduction by >95% (*32*, *38*, *39*),while having little effect on the rates of acetylene or proton reduction. Although not a good substrate for the α-195^{Gln}-substituted MoFe protein, N_2 suppresses proton reduction activity and total electron flux through nitrogenase (*32*). Thus, N_2 retains the capacity to bind at the active site of the α-195^{Gln}-substituted MoFe protein even though it cannot be effectively reduced, indicating the possibility that the α-195^{His} residue is an obligate proton donor during N_2 reduction but not for

Table 2: Hydrazine Inhibits Electron Flux and Uncouples MgATP Hydrolysis from Electron Flux

	inhibition of total electron flux by hydrazine[a]	MgATP/electron[b]	
	% electron flux remaining	proton	hydrazine
α-70^{Val}/α-195^{His}	98	2.4	2.2
α-70^{Ala}/α-195^{His}	100	2.5	2.2
α-70^{Val}/α-195^{Gln}	23	3.0	30
α-70^{Ala}/α-195^{Gln}	24	2.8	31

[a] All assays were performed at pH 7.8 and 30 °C for 10 min at a MoFe protein to Fe protein ratio of 1:20 and are reported as the percentage of electron flux remaining when hydrazine is added (electron flux to both proton and hydrazine reduction) when compared to the total electron flux under argon (total electron flux going to proton reduction). The hydrazine concentration was 50 mM in all cases where hydrazine was added. [b] The ratio of nmol of MgATP hydrolyzed/nmol of electrons passing through nitrogenase to all substrates is shown for reaction with argon (protons as substrates) and with hydrazine (protons and hydrazine as substrates).

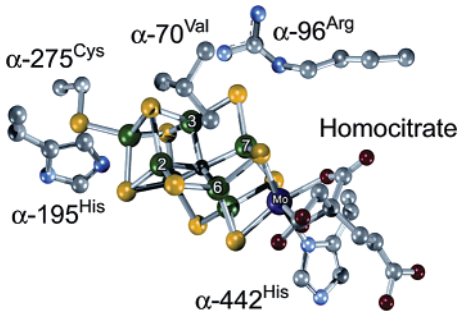

FIGURE 1: The FeMo-cofactor. A view of the FeMo-cofactor highlighting the FeS face proposed to constitute the substrate-binding site (Fe atoms 2, 3, 6, and 7) is shown along with the homocitrate and protein ligands from the MoFe protein (α-275^{Cys} and α-442^{His}). Also shown are amino acid residues near this active site face (α-70^{Val}, α-96^{Arg}, and α-195^{His}). The figure was made using the programs Viewer Pro (Accelrys Inc., San Diego, CA) and POV-Ray (Persistence of Vision, Williamstown, Australia) using the PDB file 1M1N with Fe shown in green, sulfur in yellow, molybdenum in purple, carbon in gray, oxygen in red, and nitrogen in blue.

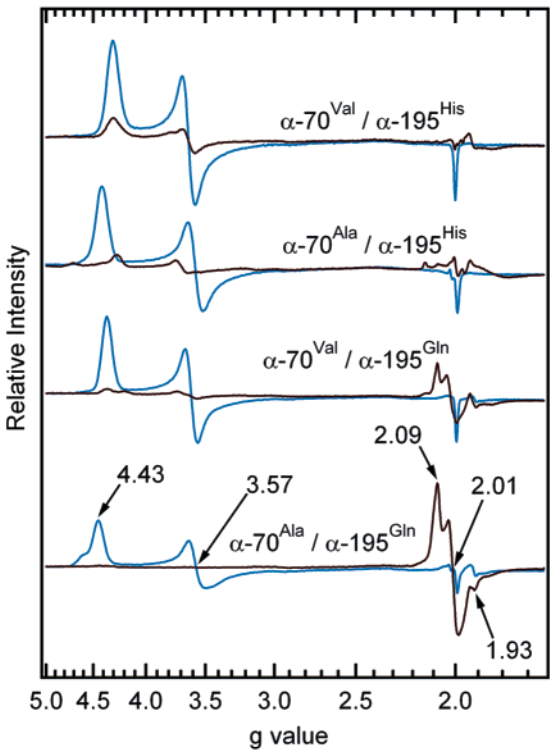

FIGURE 2: EPR spectra of nitrogenase during turnover in the presence of hydrazine. X-band EPR spectra are shown for the resting state (blue traces) and the turnover state in the presence of 50 mM hydrazine (red traces) for the wild-type (α-70^{Val}/α-195^{His}), α-70^{Ala}, α-195^{Gln}, and α-70^{Ala}/α-195^{Gln} MoFe proteins. The *g* values are noted for the resting and turnover states of the α-70^{Ala}/α-195^{Gln} MoFe protein. The MoFe protein concentration was 75 μM in all cases, and turnover and EPR parameters are described in the Experimental Procedures.

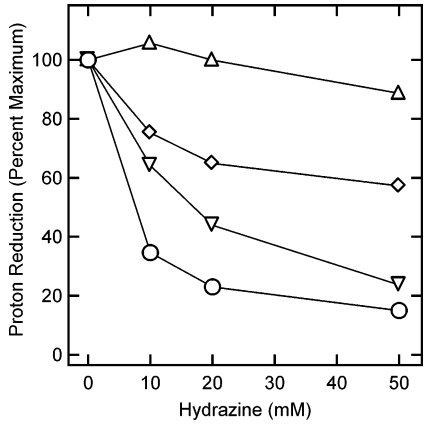

FIGURE 3: Inhibition of proton reduction activity by hydrazine in MoFe proteins. The percentage of maximal H_2 evolution activity is plotted against the concentration of hydrazine added at the initiation of the reaction for the wild-type (α-70^{Val}/α-195^{His}) (△), α-70^{Ala} (◇), α-195^{Gln} (▽), and α-70^{Ala}/α-195^{Gln} (○) MoFe proteins. Assay conditions are specified in the Experimental Procedures.

acetylene reduction. Subsequent experiments showed that a different nitrogen-containing substrate, azide, can also bind to the active site of the α-195^{Gln}-substituted MoFe protein but, like N_2, cannot be effectively reduced, indicating that α-195^{His} could be a proton donor that is specific for nitrogen-containing substrates (*40*).

Given that hydrazine is an effective substrate for the α-70^{Ala}-substituted protein, and the observed effect of the α-195^{Gln} substitution on nitrogen-containing substrates, it was of interest to determine if a doubly substituted α-70^{Ala}/α-195^{Gln} MoFe protein could be used to trap hydrazine at the active site in a highly populated state. This was a particularly attractive possibility because preliminary studies indicated that a new minor EPR-active species could be detected when the α-195^{Gln}-substituted MoFe protein was freeze-quenched under turnover conditions when hydrazine is used as substrate (Figure 2). Table 1 shows that the doubly substituted α-70^{Ala}/α-195^{Gln} MoFe protein has a much lower specific activity for hydrazine reduction when compared to the singly substituted α-70^{Ala} MoFe protein. The doubly substituted α-70^{Ala}/α-195^{Gln} MoFe protein also exhibits a relatively modest (~50%) decrease in proton reduction activity when compared to the singly substituted α-70^{Ala} MoFe protein (Table 1). The key observation is that hydrazine is a poor substrate for both the α-195^{Gln} and the doubly substituted α-70^{Ala}/α-195^{Gln} MoFe proteins, yet it is able to effectively suppress both proton reduction (Table 1) and electron flux through nitrogenase (Table 2). Importantly, the rate of MgATP hydrolysis catalyzed by these substituted MoFe proteins is comparable to the wild-type and α-70^{Ala} MoFe protein levels, indicating that hydrazine specifically blocks the reduction of protons by occupancy of the active site while having no effect on the MgATP hydrolysis rates. This is apparent from the ~15-fold increase in the MgATP/e^- ratio (ratio of nanomoles of MgATP hydrolyzed per minute per milligram to nanomoles of e^- transferred per minute per milligram) when hydrazine is added to the α-195^{Gln} and α-70^{Ala}/α-195^{Gln} MoFe proteins (Table 2). These results are the same as observed for the effect of N_2 on electron flux for the α-195^{Gln}-substituted MoFe protein (*32*) except that hydrazine more effectively suppresses proton reduction and electron flux for the doubly substituted α-70^{Ala}/α-195^{Gln} MoFe protein than does N_2 for the singly substituted α-195^{Gln} MoFe protein (*32*). The concentration dependence of hydrazine inhibition of proton reduction activity at pH 7.0 for the MoFe proteins examined here is shown in Figure 3, further illustrating hydrazine suppression of proton reduction activity in the α-195^{Gln} and α-70^{Ala}/α-195^{Gln} MoFe proteins. In aggregate, these data show that the doubly substituted α-70^{Ala}/α-195^{Gln} MoFe protein retains a capacity to bind hydrazine even though hydrazine cannot be effectively reduced, thereby inhibiting all substrate reduction activity and total electron flux. In contrast to the situation with hydrazine, the doubly substituted α-70^{Ala}/α-195^{Gln} MoFe protein is apparently unable to effectively bind or reduce N_2 because it is an extremely poor substrate and does not inhibit proton reduction (Table 1).

EPR of a Hydrazine-Trapped State. The above results indicate that hydrazine binds to the active site of the 70^{Ala}/α-195^{Gln} doubly substituted MoFe protein, thereby preventing reduction of other substrates. Because of this situation it was of interest to determine if the hydrazine-derived species bound to the FeMo-cofactor under turnover conditions could be observed by EPR spectroscopy.

The resting states of the wild-type, α-195^{Gln}, α-70^{Ala}, and α-70^{Ala}/α-195^{Gln} MoFe proteins all exhibit the characteristic $S = {}^3/_2$ EPR spectrum (with *g* values near 4.43, 3.57, 1.99) that can be assigned to the active site FeMo-cofactor (Figure 2). When the wild-type MoFe protein is trapped by freezing during the reduction of protons or hydrazine, the EPR signal from the FeMo-cofactor diminishes greatly in intensity, but

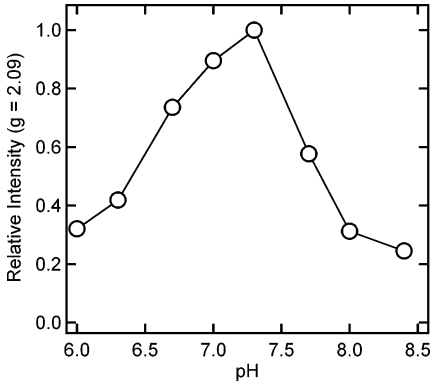

FIGURE 4: pH effect on the intensity of the hydrazine-dependent EPR signal. The pH dependence on the intensity of the $g = 2.09$ inflection for the α-70^{Ala}/α-195^{Gln} MoFe protein hydrazine trapped EPR is shown for the pH range from 6.0 to 8.4. All spectra were recorded at 10 K and 2 mW with other conditions as specified in the Experimental Procedures.

no new signals appear (Figure 2). This has been explained as accumulation of an EPR-silent FeMo-cofactor redox state. Similar behavior is observed for the α-70^{Ala} MoFe protein when trapped during the reduction of hydrazine and for the α-195^{Gln} and α-70^{Ala}/α-195^{Gln} MoFe protein variants during reduction of protons or N_2. However, when the α-195^{Gln}-substituted MoFe protein is freeze-quenched during reduction of hydrazine, a minor new $S = {}^1/_2$ EPR signal is observed ($g = [2.09, 2.01, 1.93]$). The doubly substituted MoFe protein (α-70^{Ala}/α-195^{Gln}) shows an even more complete conversion to this new EPR active state when trapped during hydrazine reduction (Figure 2). Spin integration of the hydrazine-dependent EPR signal for the α-70^{Ala}/α-195^{Gln} MoFe protein shows approximately 70% conversion of the FeMo-cofactor signal to the new EPR signal. Other minor EPR signals that are observed in the turnover spectrum can be assigned to residual reduced Fe protein.

Appearance of a new EPR signal when the α-195^{Gln}- and α-70^{Ala}/α-195^{Gln}-substituted MoFe proteins are freeze-quenched during hydrazine reduction is consistent with the kinetic results suggesting that this signal originates from hydrazine or a reduction intermediate species that is trapped on the FeMo-cofactor. As shown in Figure 4, the maximal conversion to the intermediate is achieved near pH 7.4, with higher and lower pH values resulting in a lower intensity for the EPR signal. As shown in Figure 5, the EPR signals of the intermediate and the resting state FeMo-cofactor of the α-70^{Ala}/α-195^{Gln} protein both show a Curie law temperature dependence, as expected for signals associated with ground states that are well isolated in energy from excited states. Similar temperature dependence is observed for the EPR signal of the resting state FeMo-cofactor in the wild-type MoFe protein. The dependence of the EPR signal intensities on microwave power shows that the hydrazine adduct $S = {}^1/_2$ EPR signal in the α-70^{Ala}/α-195^{Gln} MoFe protein saturates at a much lower power than does the $S = {}^3/_2$ resting-state FeMo-cofactor signal (Figure 6). The resting states of the α-70^{Ala}/α-195^{Gln} and the wild-type MoFe proteins show nearly identical microwave power dependencies.

ENDOR of a Hydrazine-Trapped State. To determine if the turnover intermediate trapped during hydrazine reduction by the α-195^{Gln} and α-70^{Ala}/α-195^{Gln} proteins indeed contains

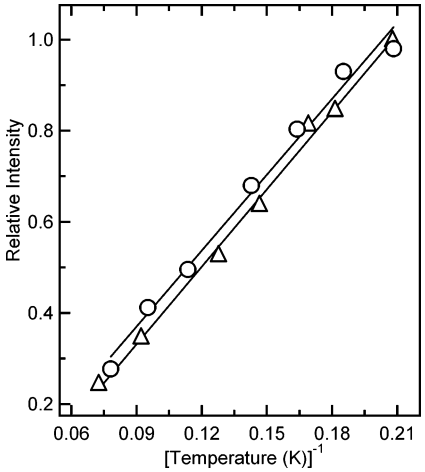

FIGURE 5: Temperature dependence of EPR signals. The relative intensity of the $g = 2.09$ inflection of the hydrazine-dependent turnover EPR signal for the α-70^{Ala}/α-195^{Gln} MoFe protein at pH 7.3 is plotted against the inverse of the temperature of the EPR measurement (○). The relative intensity of the $g = 4.43$ inflection of the resting state EPR signal for the α-70^{Ala}/α-195^{Gln} MoFe protein at pH 7.3 is also plotted against the inverse of the temperature of the EPR measurement (△). The microwave power was 100 μW for the turnover state and 200 μW for the resting state, and all other parameters were as described in the Experimental Procedures.

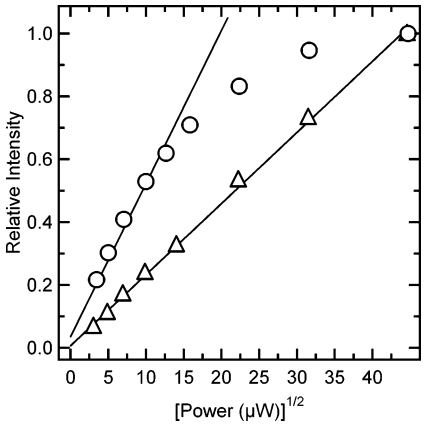

FIGURE 6: Microwave power dependence of EPR signals. The EPR signal intensity is plotted for the resting state of the α-70^{Ala}/α-195^{Gln} MoFe protein at 4.8 K ($g = 4.43$) (△) and for the hydrazine turnover state for the α-70^{Ala}/α-195^{Gln} MoFe protein at 4.8 K (inflection at $g = 2.09$) (○) against the square root of the microwave power in μW. All other parameters are as specified in the Experimental Procedures.

a hydrazine-derived species bound to the FeMo-cofactor, pulsed ENDOR experiments on freeze-quenched samples prepared with ^{14}N- or ^{15}N-labeled N_2H_4 were performed. Figure 7 presents spectra taken at the single-crystal-like field value, g_1. For the sample prepared with $^{15}N_2H_4$, the spectrum contains a single ^{15}N doublet split by the hyperfine coupling, $A(g_1) = 1.5$ MHz, and centered at the ^{15}N Larmor frequency. As this signal is absent in the spectrum of a sample prepared with $^{14}N_2H_4$, the result confirms that the intermediate indeed is derived from hydrazine and is bound to the FeMo-cofactor.

A spectrum taken at a single-crystal-like field value represents a single orientation of the paramagnetic center relative to the magnetic field, and as such the number of hyperfine-split ^{15}N doublets exhibited by the spectrum immediately corresponds to the number of *types* of ^{15}N bound to the cofactor. Thus, the single ^{15}N doublet of Figure 7

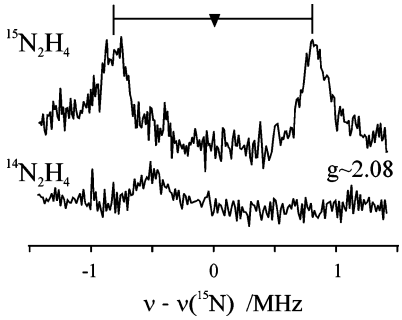

FIGURE 7: Q-band ^{15}N Mims ENDOR. ENDOR at g_1 (~2.08) of the α-70^{Ala}/α-195^{Gln} MoFe protein turnover intermediate trapped during reduction of $^{15}N_2H_4$ and $^{14}N_2H_4$. Conditions: microwave frequency, 34.856 GHz; microwave pulse width, 52 ns; $\tau = 352$ ns; rf pulse width, 60 ms; repetition rate, 70 Hz; temperature, 2 K.

suggests that the hydrazine-derived species bound to the FeMo-cofactor may have a single *type* of ^{15}N associated with it. When one scales the hyperfine coupling for that associated with a single electron in a 2s orbital, the ^{15}N coupling displayed by the intermediate is comparable to that of the C2 carbon of the previously characterized allyl alcohol species that is bound to the FeMo-cofactor (*14*) as a metallacycle intermediate when propargyl alcohol is used as a substrate for the α-70^{Ala}-substituted MoFe protein. Work in progress shows that the ^{15}N signal can be detected at fields across the EPR envelope. A full set of such spectra should provide information about both the number of types and the structure of the ^{15}N species associated with FeMo-cofactor.

DISCUSSION

To observe a nitrogenase reaction intermediate by EPR spectroscopy requires that such species actually exhibit an EPR spectrum and, if so, that it be trapped in high occupancy under turnover conditions. These requirements were recently met for the nonphysiological substrate propargyl alcohol (*14*, *20*), where hydrogen bonding between the reduction intermediate and the imidazole group of α-195^{His} was shown to stabilize the bound allyl alcohol product trapped by freezing in a highly populated state that could be detected by EPR. Nevertheless, the relevance of the species trapped when propargyl alcohol is used as a substrate to intermediates that form during N_2 reduction is not clear. Consequently, the goal of the present work was to develop a strategy for the trapping of a nitrogen-containing species that is also amenable to spectroscopic analyses. Previous work had already established that substitution of the MoFe α-195^{His} by glutamine results in an altered MoFe protein that retains an ability to bind N_2 even though N_2 is not efficiently reduced (*32*). Although a highly populated state of a bound species might actually exist when N_2 is used as substrate for the α-195^{Gln}-substituted MoFe protein, such a state is not detected by EPR under freeze−quench conditions. However, when the α-195^{His}-substituted protein was freeze-quenched under turnover conditions with hydrazine as the substrate, a new minor species could be detected by EPR (Figure 2). Because hydrazine is only a poor substrate for the wild-type enzyme and because substitution of the α-70^{Val} residue by alanine improves the capacity for hydrazine reduction, we constructed the doubly substituted α-195^{Gln}/α-70^{Ala} MoFe protein.

Freeze−quenching of the α-195^{Gln}/α-70^{Ala} MoFe protein under turnover conditions with hydrazine as substrate results in a high population (~70%) of a trapped intermediate with an $S = {}^1/_2$ EPR signal (Figure 2). This spectrum is similar to those exhibited by intermediates that form when the inhibitor CO (*11*−*13*) or the substrates CS_2 (*17*), propargyl alcohol (*14*), and acetylene (*16*) are freeze-trapped under turnover conditions. The overall line shape of the hydrazine-induced EPR spectrum reported here is similar to the EPR line shapes originating from these other bound species, although each shows a unique set of *g* values. Likewise, all of these $S = {}^1/_2$ states show more rapid microwave power saturation when compared with the $S = {}^3/_2$ resting state of the FeMo-cofactor. These observations suggest that the oxidation state of the FeMo-cofactor might be the same in all of these instances.

Of relevance to the mechanism of nitrogenous substrate reduction by nitrogenase, both hydrazine and N_2 reduction rates are significantly decreased for the α-195^{Gln} and α-70^{Ala}/α-195^{Gln} MoFe proteins. This is consistent with α-195^{His} providing protons for the reduction of both of these substrates. Given the location of α-195^{His} (Figure 1) over the FeS face composed of Fe atoms 2, 3, 6, and 7, this provides further support for the proposal that N_2 and hydrazine bind to the Fe-S face of the FeMo-cofactor approached by α-70^{Val} and α-195^{His}. Further, given the distance of α-195^{His} and α-70^{Val} away from the Mo, it is difficult to imagine how Mo could participate directly in binding either N_2 or hydrazine. The observation that both N_2 and hydrazine bind to the FeMo-cofactor in the α-195^{Gln} MoFe proteins, yet only hydrazine binding yields a new EPR active state, is consistent with the idea that the MoFe protein needs to accumulate different numbers of electrons/protons in order to bind different substrates. For example, kinetic studies indicate that the MoFe protein must accept three electrons before N_2 can bind (*41*). Assuming that all three electrons go to the FeMo-cofactor (some or all could reside on the P-cluster), then the electron count would become even after the addition of three electrons, and it is expected that the FeMo-cofactor would be in an EPR-silent state when N_2 is able to bind. This is consistent with the absence of an EPR signal under conditions where N_2 is clearly binding, as evident from the inhibition of all substrate reduction including proton reduction in the α-195^{Gln} MoFe proteins. As hydrazine reduction requires two electrons and two protons, compared to six electrons and six protons for N_2, it is reasonable to assume that hydrazine binds to a state of the MoFe protein with fewer accumulated electrons (as does acetylene). Kinetic studies suggest that acetylene binds to a two-electron reduced state of the MoFe protein relative to the resting state, whereas N_2 binds to a three- or four-electron reduced state of the MoFe protein (*41*). Assuming the two electrons reside in the FeMo-cofactor, then it is reasonable that the state that binds hydrazine could have an FeMo-cofactor that is two electrons reduced relative to the resting state, and therefore it would be expected to be EPR active. This could explain why a hydrazine-bound state is observed in the α-195^{Gln} MoFe proteins, whereas the N_2-bound state is EPR silent. The fact that different substrates access the active site at different redox states is also manifested in the nonreciprocity in their mutual inhibition parameters. It should be pointed out, however, that the formal valency state of

the FeMo-cofactor would depend on the number of electrons formally transferred to the substrate.

The observation of a ^{15}N ENDOR signal associated with the $S = {}^1/_2$ intermediate prepared with $^{15}N_2H_4$ establishes that the intermediate indeed contains a hydrazine-derived species bound to the FeMo-cofactor. The appearance of a single ^{15}N doublet (Figure 7) at the g_1 single-crystal-like field also suggests that the hydrazine-derived species bound to the FeMo-cofactor might have a single type of ^{15}N associated with it, indicating either symmetrical binding of an N−N species or binding of a hydrazine cleavage product. Detailed ENDOR studies will be required to test this possibility and to fully characterize the nature and bonding of the hydrazine-derived species.

The present studies have presented a strategy for trapping an intermediate during hydrazine reduction as a hydrazine-derived species bound to the nitrogenase active site FeMo-cofactor. Characterization of this bound intermediate should provide more details about the mechanism of reduction of this nitrogenous substrate. It is reasonable to expect that hydrazine reduction would generate states that correspond to the late stages in the N_2 reduction pathway. The initial stages of N_2 reduction will involve different intermediates and may involve different binding sites. Thus, an important research objective remains to trap and characterize intermediates generated during the actual process of N_2 reduction.

ACKNOWLEDGMENT

The authors thank Valerie Cash, Whittney Brough, and Mike Yurth for technical assistance.

REFERENCES

1. Burgess, B. K., and Lowe, D. J. (1996) The mechanism of molybdenum nitrogenase, *Chem. Rev. 96*, 2983−3011.
2. Seefeldt, L. C., Dance, I., and Dean, D. R. (2004) Substrate interactions with nitrogenase: Fe versus Mo, *Biochemistry 43*, 1401−1409.
3. Rees, D. C., and Howard, J. B. (2000) Nitrogenase: standing at the crossroads, *Curr. Opin. Chem. Biol. 4*, 559−566.
4. Shah, V. K., and Brill, W. J. (1977) Isolation of an iron−molybdenum cofactor from nitrogenase, *Proc. Natl. Acad. Sci. U.S.A. 74*, 3249−3253.
5. McLean, P. A., and Dixon, R. A. (1981) Requirement of *nifV* gene for production of wild-type nitrogenase enzyme in *Klebsiella pneumoniae*, *Nature 292*, 655−656.
6. Dance, I. (2003) The consequences of an interstitial N atom in the FeMo cofactor of nitrogenase, *Chem. Commun.*, 324−325.
7. Huniar, U., Ahlrichs, R., and Coucouvanis, D. (2004) Density functional theory calculations and exploration of a possible mechanism of N_2 reduction by nitrogenase, *J. Am. Chem. Soc. 126*, 2588−2601.
8. Hinnemann, B., and Norskov, J. K. (2003) Modeling a central ligand in the nitrogenase FeMo cofactor, *J. Am. Chem. Soc. 125*, 1466−1467.
9. Lovell, T., Liu, T., Case, D. A., and Noodleman, L. (2003) Structural, spectroscopic, and redox consequences of a central ligand in the FeMoco of nitrogenase: A density functional theoretical study, *J. Am. Chem. Soc. 125*, 8377−8383.
10. Pollock, C. R., Lee, H.-I., Cameron, L. M., DeRose, V. J., Hales, B. J., Orme-Johnson, W. H., and Hoffman, B. M. (1995) Investigation of CO bound to inhibited forms of nitrogenase MoFe protein by ^{13}C ENDOR, *J. Am. Chem. Soc. 117*, 8686−8687.
11. Christie, P. D., Lee, H. I., Cameron, L. M., Hales, B. J., Orme-Johnson, W. H., and Hoffman, B. M. (1996) Identification of the CO-binding cluster in nitrogenase MoFe protein by ENDOR of ^{57}Fe isotopomers, *J. Am. Chem. Soc. 118*, 8707−8709.
12. Lee, H. I., Cameron, L. M., Hales, B. J., and Hoffman, B. M. (1997) CO binding to the FeMo cofactor of CO-inhibited nitrogenase: ^{13}CO and ^1H Q-band ENDOR investigation, *J. Am. Chem. Soc. 119*, 10121−10126.
13. Lee, H. I., Hales, B. J., and Hoffman, B. M. (1997) Metal-ion valencies of the FeMo cofactor in CO-inhibited and resting state nitrogenase by ^{57}Fe Q-band ENDOR, *J. Am. Chem. Soc. 119*, 11395−11400.
14. Lee, H. I., Igarashi, R. Y., Laryukhin, M., Doan, P. E., Dos Santos, P. C., Dean, D. R., Seefeldt, L. C., and Hoffman, B. M. (2004) An organometallic intermediate during alkyne reduction by nitrogenase, *J. Am. Chem. Soc. 126*, 9563−9569.
15. Benton, P. M. C., Laryukhin, M., Mayer, S. M., Hoffman, B. M., Dean, D. R., and Seefeldt, L. C. (2003) Localization of a substrate binding site on FeMo-cofactor in nitrogenase: trapping propargyl alcohol with an α-70-substituted MoFe protein, *Biochemistry 42*, 9102−9109.
16. Lee, H. I., Sorlie, M., Christiansen, J., Song, R., Dean, D. R., Hales, B. J., and Hoffman, B. M. (2000) Characterization of an intermediate in the reduction of acetylene by nitrogenase α-Gln195 MoFe protein by Q-band EPR and ^{13}C, ^1H ENDOR, *J. Am. Chem. Soc. 122*, 5582−5587.
17. Ryle, M. J., Lee, H. I., Seefeldt, L. C., and Hoffman, B. M. (2000) Nitrogenase reduction of carbon disulfide: freeze-quench EPR and ENDOR evidence for three sequential intermediates with cluster-bound carbon moieties, *Biochemistry 39*, 1114−1119.
18. Mayer, S. M., Niehaus, W. G., and Dean, D. R. (2002) Reduction of short chain alkynes by a nitrogenase alpha-70Ala-substituted MoFe protein, *J. Chem. Soc., Dalton Trans. 5*, 802−807.
19. Barney, B. M., Igarashi, R. Y., Dos Santos, P. C., Dean, D. R., and Seefeldt, L. C. (2004) Substrate interaction at an iron−sulfur face of the FeMo-cofactor during nitrogenase catalysis, *J. Biol. Chem. 279*, 53621−53624.
20. Igarashi, R. Y., Dos Santos, P. C., Niehaus, W. G., Dance, I. G., Dean, D. R., and Seefeldt, L. C. (2004) Localization of a catalytic intermediate bound to the FeMo-cofactor of nitrogenase, *J. Biol. Chem. 279*, 34770−34775.
21. Dance, I. (2004) The mechanism of nitrogenase. Computed details of the site and geometry of binding of alkyne and alkene substrates and intermediates, *J. Am. Chem. Soc. 126*, 11852−11863.
22. Pickett, C. J. (1996) The Chatt cycle and the mechanism of enzymic reduction of molecular nitrogen, *J. Biol. Inorg. Chem. 1*, 601−606.
23. Thorneley, R. N. F., Eady, R. R., and Lowe, D. J. (1978) Biological nitrogen fixation by way of an enzyme-bound dinitrogen-hydride intermediate, *Nature 272*, 557−558.
24. Yandulov, D. V., and Schrock, R. R. (2003) Catalytic reduction of dinitrogen to ammonia at a single molybdenum center, *Science 301*, 76−78.
25. Fryzuk, M. D., and MacKay, B. A. (2004) Dinitrogen coordination chemistry: On the biomimetic borderlands, *Chem. Rev. 104*, 385−401.
26. Chatt, J., Dilworth, J. R., and Richards, R. L. (1978) Recent advances in the chemistry of nitrogen fixation, *Chem. Rev. 78*, 589−625.
27. Dilworth, M. J., and Eady, R. R. (1991) Hydrazine is a product of dinitrogen reduction by the vanadium−nitrogenase from *Azotobacter chroococcum*, *Biochem. J. 277*, 465−468.
28. Dilworth, M. J., Eldridge, M. E., and Eady, R. R. (1993) The molybdenum and vanadium nitrogenases of *Azotobacter chroococcum*: effect of elevated temperature on N_2 reduction, *Biochem. J. 289*, 395−400.
29. Davis, L. C. (1980) Hydrazine as a substrate and inhibitor of *Azotobacter vinelandii* nitrogenase, *Arch. Biochem. Biophys. 204*, 270−276.
30. Christiansen, J., Goodwin, P. J., Lanzilotta, W. N., Seefeldt, L. C., and Dean, D. R. (1998) Catalytic and biophysical properties of a nitrogenase apo-MoFe protein produced by a *nifB*-deletion mutant of *Azotobacter vinelandii*, *Biochemistry 37*, 12611−12623.
31. Christiansen, J., Seefeldt, L. C., and Dean, D. R. (2000) Competitive substrate and inhibitor interactions at the physiologically relevant active site of nitrogenase, *J. Biol. Chem. 275*, 36104−36107.
32. Kim, C. H., Newton, W. E., and Dean, D. R. (1995) Role of the MoFe protein alpha-subunit histidine-195 residue in FeMo-cofactor binding and nitrogenase catalysis, *Biochemistry 34*, 2798−2808.
33. Corbin, J. L. (1984) Liquid chromatographic-fluorescence determination of ammonia from nitrogenase reactions: A 2 min assay, *Appl. Environ. Microbiol. 47*, 1027−1030.

34. Dilworth, M. J., Eldridge, M. E., and Eady, R. R. Correction for creatine interference with the direct indophenol measurement of NH_3 in steady-state nitrogenase assays, *Anal. Biochem. 207*, 6−10.
35. Werst, M. M., Davoust, C. E., and Hoffman, B. M. (1991) Ligand spin densities in blue copper proteins by Q-band proton and nitrogen-14 ENDOR spectroscopy, *J. Am. Chem. Soc. 113*, 1533−1538.
36. Schweiger, A., and Jeschke, G. (2001) *Principles of Pulse Electron Paramagnetic Resonance*, Oxford University Press, Oxford, U.K.
37. Davoust, C. E., Doan, P. E., and Hoffman, B. M. (1996) Q-band pulsed electron spin−echo spectrometer and its application to ENDOR and ESEEM, *J. Magn. Reson. 119*, 38−44.
38. Fisher, K., Dilworth, M. J., and Newton, W. E. (2000) Differential effects on N_2 binding and reduction, HD formation, and azide reduction with alpha-195His- and alpha-191Gln-substituted MoFe proteins of *Azotobacter vinelandii* nitrogenase, *Biochemistry 39*, 15570−15577.
39. Fisher, K., Dilworth, M. J., Kim, C. H., and Newton, W. E. (2000) *Azotobacter vinelandii* nitrogenases containing altered MoFe proteins with substitutions in the FeMo-cofactor environment: effects on the catalyzed reduction of acetylene and ethylene, *Biochemistry 39*, 2970−2979.
40. Dilworth, M. J., Fisher, K., Kim, C. H., and Newton, W. E. (1998) Effects on substrate reduction of substitution of histidine-195 by glutamine in the alpha-subunit of the MoFe protein of *Azotobacter vinelandii* nitrogenase, *Biochemistry 37*, 17495−17505.
41. Thorneley, R. N. F., and Lowe, D. J. (1996) Nitrogenase: Substrate binding and activation, *J. Biol. Inorg. Chem. 1*, 576−580.

BI0504409